Hindawi Publishing Corporation
International Journal of Photoenergy
Volume 2012, Article ID 631435, 9 pages
doi:10.1155/2012/631435

Research Article

Preparation and Characterization of Visible-Light-Activated Fe-N Co-Doped TiO_2 and Its Photocatalytic Inactivation Effect on Leukemia Tumors

Kangqiang Huang,[1] Li Chen,[2] Jianwen Xiong,[1] and Meixiang Liao[3]

[1] *Laboratory of Quantum Information Technology, School of Physics and Telecommunication Engineering, South China Normal University, Guangzhou 510006, China*
[2] *Department of Physics and Optoelectronic Engineering, Guangdong University of Technology, Guangzhou 510006, China*
[3] *School of Physics and Engineering, Sun Yat-Sen University, Guangzhou 510275, China*

Correspondence should be addressed to Jianwen Xiong, jwxiong@scnu.edu.cn

Received 16 January 2012; Revised 19 February 2012; Accepted 19 February 2012

Academic Editor: Baibiao Huang

The Fe-N co-doped TiO_2 nanocomposites were synthesized by a sol-gel method and characterized by scanning electron microscope (SEM), transmission electron microscope (TEM), X-ray diffraction (XRD), ultraviolet-visible absorption spectroscopy (UV-vis) and X-ray photoelectron spectroscopy (XPS). Then the photocatalytic inactivation of Fe-N-doped TiO_2 on leukemia tumors was investigated by using Cell Counting Kit-8 (CCK-8) assay. Additionally, the ultrastructural morphology and apoptotic percentage of treated cells were also studied. The experimental results showed that the growth of leukemic HL60 cells was significantly inhibited in groups treated with TiO_2 nanoparticles and the photocatalytic activity of Fe-N-TiO_2 was significantly higher than that of Fe-TiO_2 and N-TiO_2, indicating that the photocatalytic efficiency could be effectively enhanced by the modification of Fe-N. Furthermore, when 2 wt% Fe-N-TiO_2 nanocomposites at a final concentration of 200 μg/mL were used, the inactivation efficiency of 78.5% was achieved after 30-minute light therapy.

1. Introduction

Titanium dioxide (TiO_2) as photocatalyst has been widely used for industrial and medical applications due to its useful physical and biological properties in the last two decades, such as disposal of wastewater, decontamination of air pollutants, and sterilization of bacteria [1–4]. It has been well known that photoinduced electrons and holes could be generated on the TiO_2 surface under exposure to ultraviolet (UV) light [5, 6]. These excited electrons and holes have strong reduction and oxidation activities and could further react with hydroxyl ions or water resulting in the formation of various reactive oxygen species (ROS) which have been proved to significantly damage cancer cells [7–9].

Recently, with the rapid development of nanotechnology, research involving use of TiO_2 nanoparticle in biomedical fields has also drawn attention [10, 11]. TiO_2 for phototherapy of cancer cells has been noticed [12–15]. Therefore, TiO_2 nanoparticle in this case is regarded as a potential anticancer drug or photosensitizer for photodynamic therapy (PDT) to improve the traditional photodynamic effect. However, TiO_2 was only excited by UVlight due to its wide band gap (approximately 3.2 eV). Additionally, the photogenerated holes are easy to recombine with the photoinduced electrons, which greatly reduce the photocatalytic efficiency of TiO_2 nanoparticles and hinder its practical applications [16–19]. Fortunately, it has been demonstrated that the visible light absorption and photocatalytic activity of TiO_2 can be effectively improved by the method of metal or nonmetal elements doping [20–24]. We aim to enhance the photocatalytic inactivation efficiency of TiO_2 on tumor cells by the modification of Fe-N.

In the present work, Fe-N-doped TiO_2 nanocomposites were used as a "photosensitizer" of PDT for tumor treatment in vitro. Up to our knowledge, there are still no previous reports on the study of photocatalytic inactivation effects of

Fe-N-doped TiO_2 on leukemia HL60 cells. The aims of the present study were focused on the possible use of co-doped TiO_2 as an anticancer agent in the presence of visible light and its potential therapeutic effect on leukemia-tumor-based PDT.

2. Materials and Methods

2.1. Chemicals and Apparatus. HL60 cells were kindly provided by the Department of Medicine of Sun Yat-Sen University. Fluo-3 AM was purchased from Sigma (USA). Cell Counting Kit-8 (CCK-8) assays were purchased from Dojindo (Japan). RPMI medium 1640 was obtained from Gibco BRL (USA). All chemicals used were of the highest purity commercially available. The stock solutions of the compounds were prepared in serum-free medium immediately before using in experiments.

These apparatuses, including ZEISS Ultra-55 scanning electron microscope (Carl Zeiss, Germany), JEM-2100HR transmission electron microscope (JEOL, Japan), BRUKER D8 ADVANCE X-ray powder diffractometer (XRD) (Bruker, Germany), U-3010 UV-visible spectrophotometer (Hitachi, Japan), AXIS Ultra X-ray photoelectron spectroscopy (XPS) (Kratos, UK), the Countess Automated Cell Counter (Invitrogen, USA), a photodiode (Hitachi, Japan), Model 680 Microplate Reader (Bio-Rad, USA), HH.CP-TW80 CO_2 incubator, and PDT reaction chamber, were used.

2.2. Preparation of Fe-N Co-Doped TiO_2 Nanocomposites Solutions. The 2 wt% Fe-N-TiO_2 nanocomposites were synthesized using sol-gel method [25, 26]. Firstly, 19 mL of tetrabutyl titanate (55.6 mmol) and 0.32 g $Fe(NO_3)_2$ (0.4 mmol was dissolved in 60 mL of anhydrous ethanol at room temperature to prepare solution A. Meanwhile, the appropriate amount of hydroxylamine hydrochloride was mixed with 2 mL of doubly distilled water and 16 mL of anhydrous ethanol to prepare solution B. Afterwards, solution A was slowly added to solution B at a rate of 2 mL per minute under vigorous stirring within 10 min. The solution was subsequently stirred for further 30–60 min. The prepared TiO_2 gels after washing with deionized water were dried at 120°C for 12 h. The 2 wt% Fe-N co-doped TiO_2 nanocomposites were obtained after calcination at 400°C for 2 h and finally grinded for 15 min. Additionally, the pure TiO_2, 2 wt% Fe-TiO_2, and 2 wt% N-TiO_2 were prepared through a similar procedure.

The prepared samples were encapsulated in four bottles, respectively, and then placed in YX-280B-type pressure steam sterilizer to sterilize for 30 minutes. Finally, an appropriate amount of culture medium was added to fully dissolve the nanoparticles. All solutions were filtered through a 0.22 μm membrane filter and stored in the dark at 4°C before being used in the experiments.

2.3. Cell Culture. Human leukemia HL60 cells were cultured in RPMI 1640 medium supplemented with 10% fetal bovine serum (FBS) in a humidified incubator with 5% CO_2 at 37°C. The cell concentration was measured using a countess automated cell counter and adjusted to the required final concentration. Cells viability before treatment was always over 95%.

2.4. Cell Viability Assay. The immediate cytotoxicity of the HL60 cells after treatment was assessed using the trypan blue exclusion test. The viable/dead cells were counted using a countess automated cell counter. Viability for the samples were further evaluated by Cell Counting Kit-8 assays (CCK-8 assay). Cell suspension (200 μL) was seeded onto 96-well plate and incubated with 20 μL CCK-8 solution at 37°C in a humidified 5% CO_2 atmosphere. After 4 h incubation, the absorbance (OD values) at 490 nm was determined using the Model 680 Microplate Reader. The percentage of viability was determined by comparison with untreated cells.

2.5. Statistical Analysis. Data are presented as means ± SD (standard deviation) from at least three independent experiments. Statistical analysis was then performed using the statistical software SPSS11.5, and values of $P < 0.05$ were considered statistically significant.

3. Results and Discussion

3.1. Characterization of Fe-N-TiO_2 Nanocomposites

3.1.1. SEM and TEM Studies. The morphology and particle size of the pure TiO_2 and Fe-N co-doped TiO_2 nanocomposites were observed with a scanning electron microscope. TEM analysis was also performed using a JEM-2100HR microscope to obtain further information and support SEM results.

The morphologies of pure $TiO_2$and Fe-N-TiO_2 prepared by sol-gel method at 400°C are shown in Figure 1. It can be seen that the average size of pure TiO_2 particles is significantly larger than that of Fe-N-TiO_2 (Figures 1(a) and 1(b)). It appears that the Fe-N-TiO_2 particles are spherical or square shaped with a primary particle size of from 18 to 20 nm.

Figures 1(c) and 1(d) display the TEM images of controlled TiO_2 and Fe-N-doped TiO_2. As shown in Figure 1(d), the particle size of most of Fe-N-doped TiO_2 samples is approximately 19.0 nm, which is basically consistent with the SEM observation. Furthermore, with careful observation we can find that there are some fuscous points on the doped sample surfaces; maybe this can be explained by the fact that Fe and N have been successfully incorporated into the lattice of TiO_2 structure.

3.1.2. X-Ray Diffraction. XRD was used to further investigate the crystalline structural properties of the Fe-N-doped TiO_2, and the XRD patterns of TiO_2, 2wt% Fe-TiO_2, 2wt%N-TiO_2, 2wt%Fe-N-TiO_2 are presented in Figure 2.

Figure 2 shows that the four synthesized samples have the highest diffraction peak in (101) crystal plane (2θ = 25.3°), and the other diffraction peaks are consistent with crystalline phases of (004), (200), (105), (211), and (204). Thus, the doped TiO_2 nanocomposites obtained by the sol-gel method have primarily the anatase phase. Additionally,

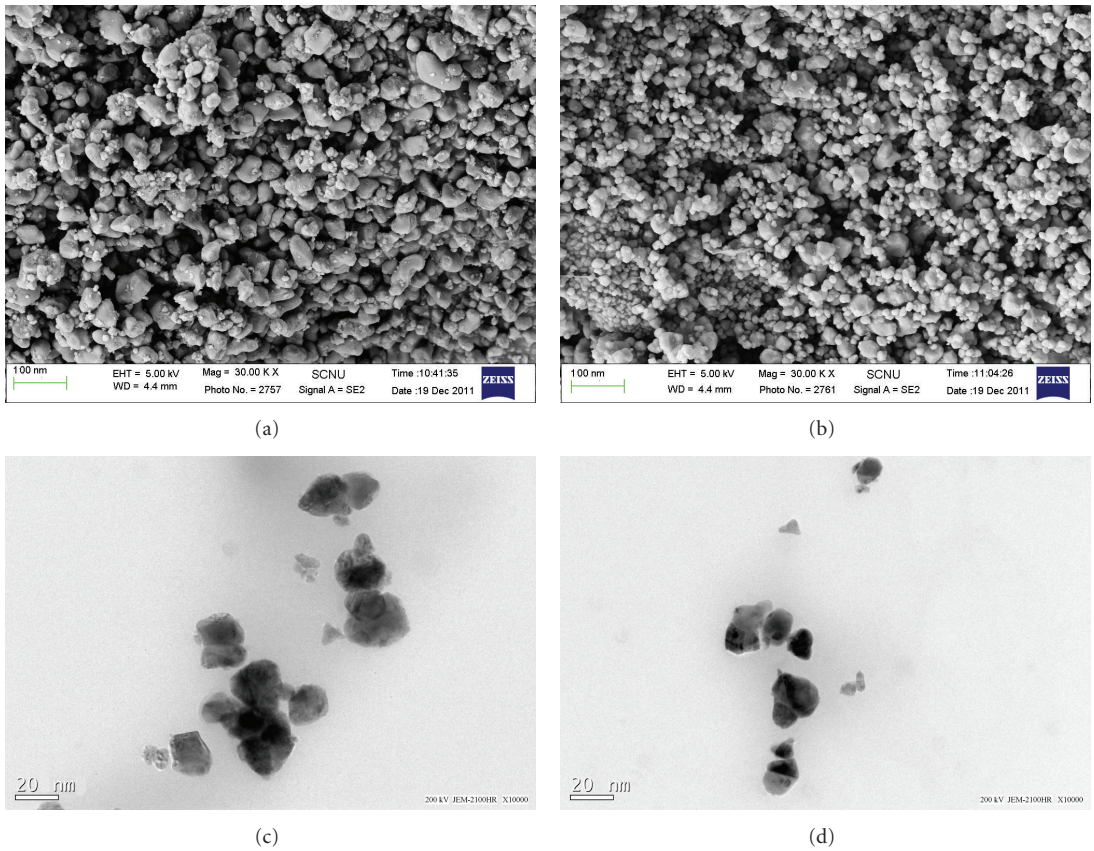

Figure 1: The SEM and TEM images of TiO_2 particles. (a) and (c): pure TiO_2; (b) and (d): 2 wt% Fe-N-TiO_2.

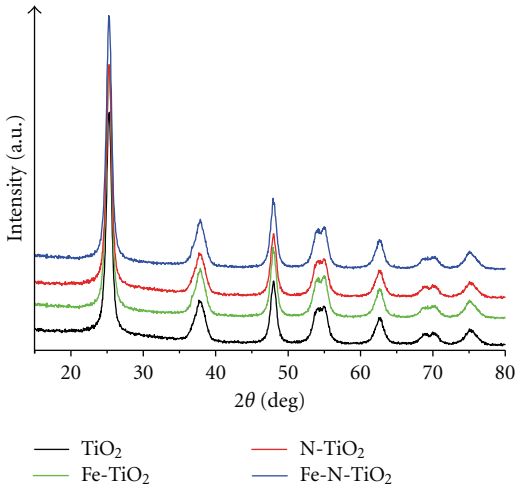

Figure 2: The XRD patterns of pure and doped TiO_2 calcined at 400°C.

compared to the undoped TiO_2, there are no indications of peaks corresponding to Fe or N observed; the reason may be attributed to the amount of Fe and N being little and well dispersed in the TiO_2 surface. Furthermore, the average crystallite sizes of the samples were roughly estimated using Scherer's equation [27], and the obtained sizes are approximately 21.5 nm, 20.7 nm, 21.0 nm, and 19.3 nm for pure TiO_2, Fe-doped TiO_2, N-doped TiO_2, and Fe-N-doped TiO_2, respectively. As can be seen from the values, the crystallite sizes of Fe-N-doped TiO_2 are smaller than those of others, indicating that Fe-N-doped TiO_2 nanocomposites are highly crystallized which is in good accordance with the results of the TEM shown in Figure 1.

3.1.3. UV-Vis Spectroscopy. The Fe-N-TiO_2 nanocomposites have been also identified with UV-vis adsorption spectra. As is shown in Figure 3, the spectrum obtained from the controlled TiO_2 has a sharp absorption edge at 393 nm due to its intrinsic band gap showing that absorption only in the ultraviolet light region (less than 400 nm). However, the absorption thresholds of the doped TiO_2 are slightly shifted towards the visible region of the spectrum. These results demonstrate that the absorption for the doped TiO_2 in the visible light region is significantly enhanced compared with that of pure TiO_2. Additionally, as can be seen in Figure 3, the onset of absorption edge of Fe-N-doped TiO_2 is extended from 393 nm to visible range 425 nm, indicating that the visible light absorption of TiO_2 nanoparticles has been effectively enhanced by the incorporation of Fe and N, which in turn may considerably increase the photocatalytic activity of TiO_2 under visible light irradiation.

In order to reach a high photocatalytic inactivation efficiency, a built lamp with many high-power light-emitting

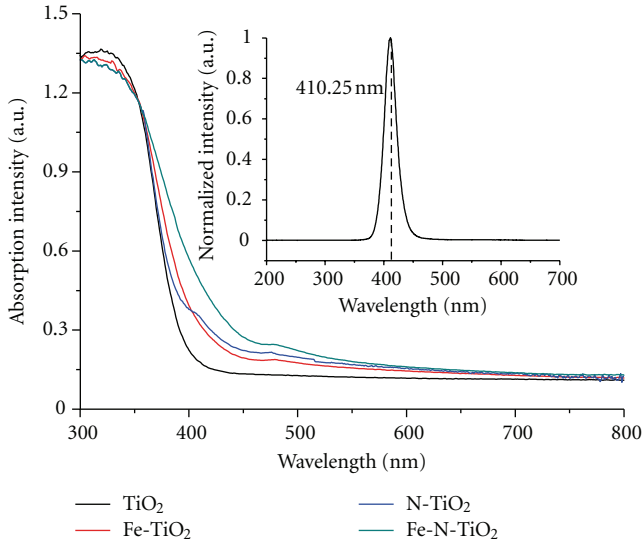

Figure 3: The UV-vis absorption spectra of TiO_2 with different doping. Inset is the normalized emission spectra of the blue LEDs.

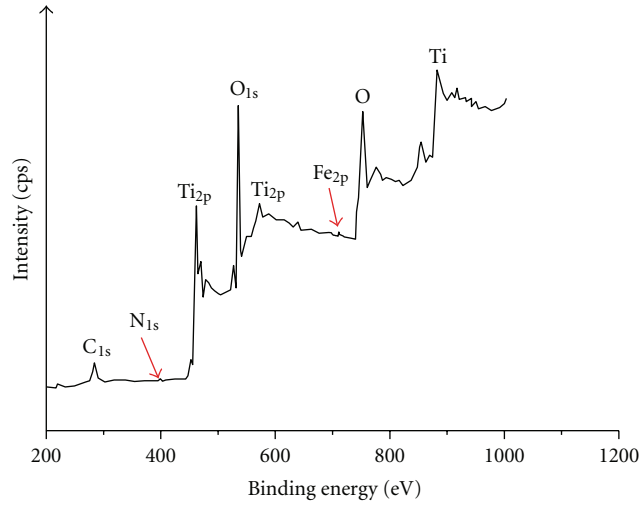

Figure 4: The XPS spectra of 2 wt% Fe-N-TiO_2 nanocomposites calcined at 400°C.

diodes (LEDs), emitting light in the visible-light region (390–425 nm) with a peak at 410.25 nm, was used as light sources. The light density at the position of the sample was 5 mW/cm^2 as measured with a photodiode. As shown in the inset, the blue LEDs can better meet the needs of the following experiments.

3.1.4. XPS Analysis. To determine whether the implementation of Fe-N co-doping is successful, the surface of Fe-N-TiO_2 nanocomposites has been investigated using XPS analysis. As it can be observed from Figure 4, the signal for Fe with a weaker peak at 710.5 eV was observed, and the binding energies in the range 710–712 eV were assigned to Fe2p3/2 of Fe^{3+} cation. The results indicate that the presence of Fe is in the form of Fe^{3+} by replacing Ti^{4+} in

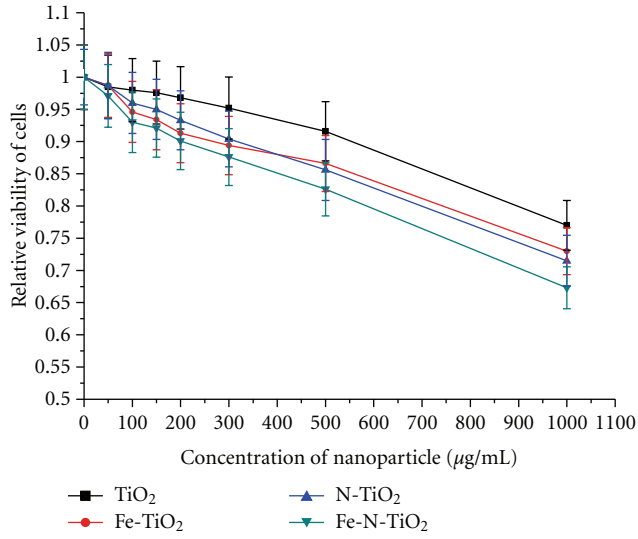

Figure 5: The influence of Fe-N-TiO_2 concentrations on the relative viability of HL60 cells. Data are presented as the means ± SD from five independent measurements. $^*P$ values are less than 0.05 as compared with untreated control cells.

the doped photocatalyst, which may cause a change in the charge distribution of the atoms on the photocatalyst surface and resulting in enhancing the photocatalytic activity. We can also find the characteristic peak at 399.7 eV which is corresponding to N_{1s}. It has been clearly determined that the Fe and N have already been incorporated into Fe-N-TiO_2 nanocomposites. Additionally, the concentrations of Fe and N, determined by XPS, of the Fe-N-TiO_2 are 0.91 wt% and 0.97 wt%, respectively, which is basically consistent with the theoretical expectation.

3.2. Cytotoxicity of TiO_2 Nanoparticles or Doped TiO_2 Nanocomposites on Leukemia Tumor Cells. It is well known that the photosensitive drugs used for cancer treatment not only have high photocatalytic inactivation capability under light irradiation, but also have no toxicity in the dark. Therefore, it is very important to investigate the cytotoxicity of TiO_2 nanocomposites without light treatment. The toxicity of Fe-N-TiO_2 was measured by exposing HL60 cells in the medium containing various concentrations of Fe-N-TiO_2 (0 μg/mL, 50 μg/mL, 100 μgl/mL, 150 μg/mL, 200 μg/mL, 300 μg/mL, 500 μgl/mL, 1000 μg/mL) for 48 hours in dark, respectively. The obtained OD values of HL60 cells at different concentrations were normalized by the OD values of control group (the final concentration of nanoparticles was 0 μg/mL). The relative viability of HL60 cells is presented in Figure 5.

As shown in Figure 5, the relative viabilities of the groups in the presence of TiO_2 or doped TiO_2 are obviously lower than those of the control group (0 μg/mL) under the same conditions, indicating that TiO_2 or doped TiO_2 has a certain degree of inhibitory or toxic effects on the proliferation of HL60 cells. Moreover, the inhibition effect of Fe-N-TiO_2 nanocomposites on HL60 cells is much more obvious than that of the other three TiO_2.

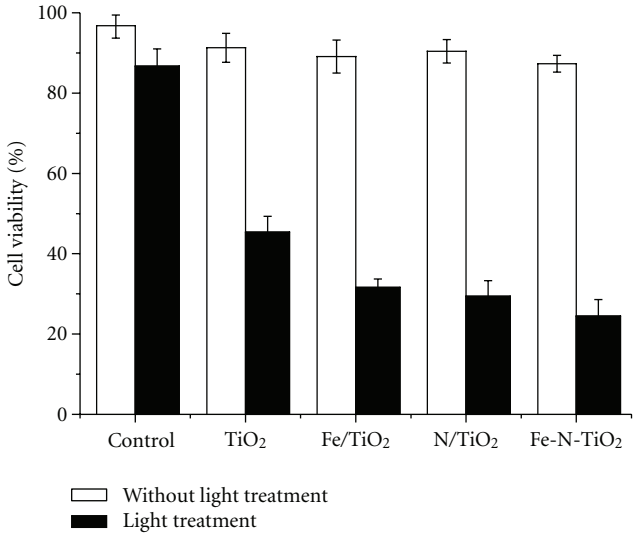

FIGURE 6: The effect of light irradiation on cell viability at an intensity of 5.0 mW/cm^2 for 30 minutes in the presence of TiO_2 or doped TiO_2. Each data point represents mean ± SD ($n = 3$). $^*P < 0.05$.

Figure 5 also shows that with the increasing concentration of nanoparticles, the viability of HL60 cells is decreased gradually. At a concentration of 1000 μg/mL, the four relative viabilities of HL60 cells for TiO_2, Fe-TiO_2, N-TiO_2, and Fe-N-TiO_2 have decreased to 77%, 73%, 71.5%, and 67.3%, respectively. However, when the concentrations of TiO_2 nanoparticles or doped-TiO_2 nanocomposites were in the range from 0 to 200 μg/mL, the survival rates of HL60 cells were always greater than 90%. In this case, the TiO_2 nanoparticles and doped TiO_2 nanocomposites could be considered as nontoxic materials for cancer cells in the dark, which is in agreement with the suggestions reported in references [28, 29].

3.3. Photocatalytic Inactivation Effect of Fe-N-TiO_2 Nanocomposites on Leukemia Tumor Cells. The HL60 cells were inoculated into two 96-well plates marked with A or B. The cell suspensions of plate A were exposed to light after incubating for 24 hours and then preincubated for another 24 hours in the dark. The HL60 cells in plate B were incubated for 48 hours in the incubator without light treatment. The final concentration of TiO_2or doped TiO_2 used was 200 μg/mL. The photocatalytic effect of Fe-N-TiO_2 nanocomposites on leukemic HL60 cells was evaluated by measuring OD values. The cell viability was calculated as follows:

$$\text{cell viability (\%)} = \left(\frac{\text{OD}_{\text{treated}}}{\text{OD}_{\text{untreated}}}\right) \cdot 100\%, \quad (1)$$

where the $\text{OD}_{\text{treated}}$ and $\text{OD}_{\text{untreated}}$ are the mean absorption values at 490 nm for the treated and untreated samples, respectively. The obtained results are summarized in Figure 6.

As can be observed in Figure 6, when the cells were treated with TiO_2 alone or with light irradiation alone, cell viability was basically unchanged as compared to untreated ones. However, treating cells with the combination of TiO_2 and light exposure resulted in significant decrease in cell viability compared with the control ones. It can also be found that the viability of HL60 cells in the presence of doped TiO_2 is significantly lower than that of TiO_2 after light treatment. These results reveal that the modification of Fe or N can greatly enhance the photocatalytic inactivation effect of TiO_2. Additionally, the Fe-N-doped TiO_2 nanocomposites present a higher efficiency in photokilling HL60 cancer cells compared with that of Fe-TiO_2 or N-TiO_2 under the same conditions. When 200 μg/mL Fe-N-TiO_2 (2 wt%) nanocomposites were used, the inactivation efficiency of HL60 cells can be increased to 78.5% after a 30-minute irradiation.

3.4. Ultrastructural Morphology of the Treated Cells. After light treatment (PDT), the treated cells were fixed in 2.5% glutaraldehyde in 0.1 M phosphate buffer (pH 7.4) for 1 h. They were then washed three times thoroughly with triple-distilled water before being freeze-dried using K750 turbo freeze drier. The samples were coated with platinum using automatic high-vacuum coating system (Quorum Q150T ES) before observing with a ZEISS Ultra-55 scanning electron microscope.

The ultrastructural morphology of the HL60 cells exposed to light at an intensity of 5.0 mW/cm^2 for 30 minutes in the presence Fe-N-TiO_2 nanocomposites is shown in Figure 7. Untreated control cells show numerous microvilli on their membrane surface (Figure 7(a)), whereas the cells exposed to light in the presence of Fe-N-TiO_2 nanocomposites display a markedly reduced number of microvilli compared with control cells (Figure 7(b)). The treated cells were seriously damaged with apparent deformation; some papillous protuberances are observed on the surface of cells where the cytoplasm seemed to have extruded through the membrane boundary.

3.5. Apoptosis Detection Based on the Induction of Fe-N-TiO_2 Nanocomposites. To determine whether the observed reduced cell viability is related to apoptotic cell death, we investigated apoptotic cells after 24 h treatment by the number and the sizes of dead cells obtained from the cell counter in combination with the nondestructive testing methods [30].

The obtained data are shown in Figure 8; no significant difference in the number of apoptotic cells was observed with light treatment alone and Fe-N-TiO_2 alone compared with control untreated cells. The percentage of apoptotic cells after light therapy at an intensity of 5.0 W/cm^2 for 30 minutes in the presence of Fe-N-TiO_2 was 7.3 times greater than that of control untreated cells. The results revealed that reduced cell viability was the result of apoptotic induction, which are in agreement with recent publications reporting that TiO_2 nanoparticles induce death by apoptosis in different types of cells [31, 32].

3.6. Alteration of Ca^{2+} in HL60 Cells during Light Treatment. The treated cells were incubated with Fluo-3-AM at a concentration of 500 μmol/L for 30 min. They were then

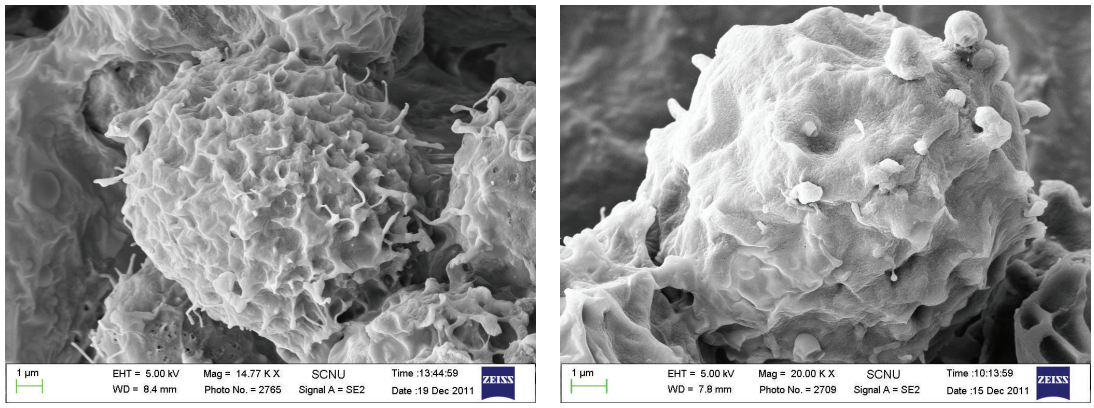

(a) (b)

Figure 7: The ultrastructural morphology of the cultured HL60 cells before and after light therapy. (a) The control cells. (b) The treated cells.

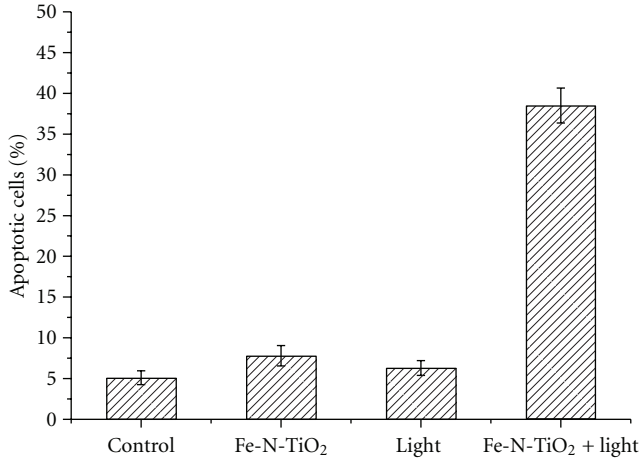

Figure 8: Change of percentage of apoptotic cells after light therapy at an intensity of 5.0 mW/cm^2 for 30 minutes in the presence of Fe-N-TiO_2. Each data point represents mean ± SD ($n = 3$). $^*P < 0.05$.

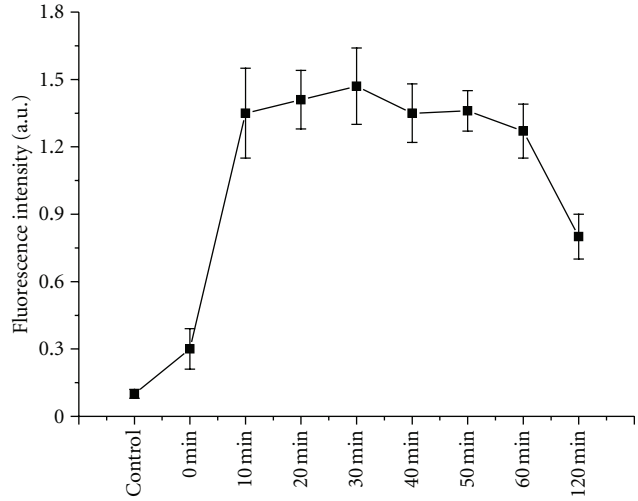

Figure 9: Alteration of Ca^{2+} in HL60 cells with Fe-N-TiO_2 nanocomposites during light therapy. Each data point represents mean ± SD ($n = 3$). $^*P < 0.05$.

washed three times with PBS before being detected using fluorescence spectrometer. The change of Ca^{2+} in HL60 cells during light treatment is presented in Figure 9.

It is now well established that cell apoptosis is executed by the family of caspases, and the activation of Ca^{2+} contributes to the morphological and functional changes associated with apoptosis [33, 34]. As can be observed from Figure 9, Ca^{2+} concentration in cells rapidly increased at the beginning of 10-minute and reached the maximum after 30-minute light treatment in the presence of Fe-N-TiO_2. It also can be found that there were no significant changes in Ca^{2+} concentration during the time from 10 minutes to 60 minutes. Moreover, according to our previous studies, the most efficient inactivation of Fe-N-TiO_2 nanocomposites on HL60 cells is located at the time of 30 minutes, which suggests that the increased concentration of Ca^{2+} promotes cell apoptosis through activation of apoptosis signaling pathways, to a certain extent.

3.7. Mechanism of Photocatalysis in Fe-N-TiO_2 Nanocomposites. The photocatalytic mechanisms of Fe-N-TiO_2 nanocomposites are initiated by the absorption of the photon hv_4 with energy lower than the band gap of TiO_2 (3.2 eV for the anatase phase), and photoinduced electrons and holes could be produced on the surface of TiO_2 as schematized in Scheme 1. An electron is promoted to the conduction band (CB) while a positive hole is formed in the valence band (VB). Excited-state electrons can reduce the dissolved O_2 to produce the superoxide anion O^-. Meanwhile, the photo-generated holes in the valence band can further react with water to generate powerful hydroxyl radicals ($OH^\bullet$) and other oxidative radicals, which are playing an important role in destroying the membrane and component of tumor cells [35, 36]. Additional benefit of the dispersion of Fe-N is the improved trapping of electrons to inhibit electron-hole recombination during irradiation, as suggested in [37–39]. Decrease of charge carriers recombination results in

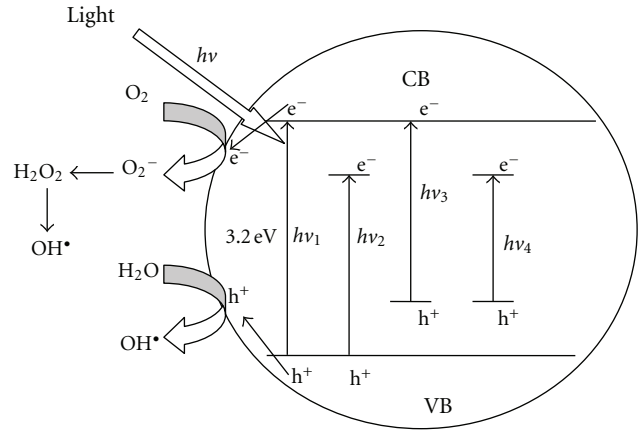

Scheme 1: Schematic representation of the mechanism of photocatalytic titanium dioxide particles (TiO_2: hv_1,Fe-TiO_2: hv_2, N-TiO_2: hv_3, Fe-N-TiO_2: hv_4).

significantly enhanced photocatalytic activity of TiO_2 nanoparticles.

4. Conclusion

In this paper, Fe-N-TiO_2 nanocomposite has been successfully synthesized by sol-gel method and for the first time used as a new "photosensitizer" in photodynamic therapy for cancer cell treatment. Then they were characterized by scanning electron microscope (SEM), transmission electron microscope (TEM), X-ray diffraction (XRD), UV-vis adsorption spectra, and X-ray photoelectron spectroscopy (XPS), respectively. Additionally, the ultrastructural morphology of treated cells and alteration of Ca^{2+} in cells during PDT were also studied. The experimental results show that the absorption of TiO_2 nanoparticles in the visible light region could be enhanced effectively by the method of (Fe, N) codoping, and both pure TiO^{2+} and doped TiO_2 nanocomposites at high concentrations have a significant inhibition on the growth of HL60 cells. It is also found that Fe-N-TiO_2 nanocomposites present much higher inactivation efficiency in photokilling HL60 cancer cells than TiO_2 nanoparticles under the same conditions, indicating that the photocatalytic inactivation effects of TiO_2 could be greatly improved by the modification of Fe-N. Moreover, the PDT efficiency of Fe-N-TiO_2 nanocomposites on HL60 cells can reach 78.5% at a concentration of 200 μg/mL after a 30-minute light treatment. The high photocatalytic inactivation effects of Fe-N-TiO_2 nanocomposites on tumor cells suggest that it may be an important potential photosensitizer-based photodynamic therapy for cancer treatment [40–42].

Acknowledgments

This work has been financially supported by the National Natural Science Foundation of China (61072029), the Natural Science Foundation of Guangdong Province (10151063101000025), and Science and Technology Planning Project of Guangzhou City (2010Y1-C111).

References

[1] K. Esquivel, L. G. Arriaga, F. J. Rodriguez, L. Martinez, and L. A. Godinez, "Development of a TiO_2 modified optical fiber electrode and its incorporation into a photoelec-trochemical reactor for wastewater treatment," *Water Research*, vol. 43, no. 14, pp. 3593–3603, 2009.

[2] M. Guarino, A. Costa, and M. Porro, "Photocatalytic TiO_2 coating-to reduce ammonia and greenhouse gases concentration and emission from animal husbandries," *Bioresource Technology*, vol. 99, no. 7, pp. 2650–2658, 2008.

[3] Y. H. Tsuang, J. S. Sun, Y. C. Huang, C. H. Lu, W. H. S. Chang, and C. C. Wang, "Studies of photokilling of bacteria using titanium dioxide nanoparticles," *Artificial Organs*, vol. 32, no. 2, pp. 167–174, 2008.

[4] C. L. Cheng, D. S. Sun, W. C. Chu et al., "The effects of the bacterial interaction with visible-light responsive titania photocatalyst on the bactericidal performance," *Journal of Biomedical Science*, vol. 16, no. 1, pp. 1–7, 2009.

[5] T. Zubkoy, D. Stahl, T. L. Thompson, D. Panayotov, O. Diwald, and J. T. Yates, "Ultraviolet light-induced hydrophilicity effect on TiO_2(110) (1-1). Dominant role of the photooxidation of adsorbed hydrocarbons causing wetting by water droplets," *Journal of Physical Chemistry B*, vol. 109, no. 32, pp. 15454–15462, 2005.

[6] J. Wang, Y. Guo, B. Liu et al., "Detection and analysis of reactive oxygen species (ROS) generated by nano-sized TiO_2 powder under ultrasonic irradiation and application in sonocatalytic degradation of organic dyes," *Ultrasonics Sonochemistry*, vol. 18, no. 1, pp. 177–183, 2011.

[7] N. Shimizu, C. Ogino, M. F. Dadjour, K. Ninomiya, A. Fujihira, and K. Sakiyama, "Sonocatalytic facilitation of hydroxyl radical generation in the presence of TiO_2," *Ultrasonics Sonochemistry*, vol. 15, no. 6, pp. 988–994, 2008.

[8] Y. Chihara, K. Fujimoto, H. Kondo et al., "Anti-tumor effects of liposome-encapsulated titanium dioxide in nude mice," *Pathobiology*, vol. 74, no. 6, pp. 353–358, 2007.

[9] J. Yu, L. Qi, and M. Jaroniec, "Hydrogen production by photocatalytic water splitting over Pt/$TiO2_2$ nanosheets with exposed (001) facets," *Journal of Physical Chemistry C*, vol. 114, no. 30, pp. 13118–13125, 2010.

[10] E. A. Rozhkova, I. Ulasov, B. Lai, N. M. Dimitrijevic, M. S. Lesniak, and T. Rajh, "A high-performance nanobio photocatalyst

for targeted brain cancer therapy," *Nano Letters*, vol. 9, no. 9, pp. 3337–3342, 2009.

[11] C. M. Sayes, R. Wahi, P. A. Kurian et al., "Correlating nanoscale titania structure with toxicity: a cytotoxicity and inflammatory response study with human dermal fibroblasts and human lung epithelial cells," *Toxicological Sciences*, vol. 92, no. 1, pp. 174–185, 2006.

[12] J. Xu, Z. D. Chen, Y. Sun, C. M. Chen, and Y. Z. Jiang, "Photocatalytic killing effect of gold-doped TiO_2 nanocomposites on human colon carcinoma LoVo cells," *Acta Chimica Sinica*, vol. 66, no. 10, pp. 1163–1167, 2008.

[13] J. J. Wang, B. J. S. Sanderson, and H. Wang, "Cyto- and genotoxicity of ultrafine TiO_2 particles in cultured human lymphoblastoid cells," *Mutation Research*, vol. 628, no. 2, pp. 99–106, 2007.

[14] Y. S. Lee, S. Yoon, H. J. Yoon et al., "Inhibitor of differentiation 1 (Id1) expression attenuates the degree of TiO_2-induced cytotoxicity in H1299 non-small cell lung cancer cells," *Toxicology Letters*, vol. 189, no. 3, pp. 191–199, 2009.

[15] K. Q. Huang, L. Chen, M. X. Liao, and J. W. Xiong, "The photocatalytic inactivation effect of fe-doped TiO_2 nanocomposites on leukemic HL60 cells based photodynamic therapy," *International Journal of Photoenergy*, vol. 2012, Article ID 367072, 12 pages, 2012.

[16] J. Xu, Y. Sun, J. Huang et al., "Photokilling cancer cells using highly cell-specific antibody-TiO_2 bioconjugates and electroporation," *Bioelectrochemistry*, vol. 71, no. 2, pp. 217–222, 2007.

[17] H. Choi, E. Stathatos, and D. D. Dionysiou, "Sol-gel preparation of mesoporous photocatalytic TiO_2 films and TiO_2/Al_2O_3 composite membranes for environmental applications," *Applied Catalysis B*, vol. 63, no. 1-2, pp. 60–67, 2006.

[18] J. Yu, Y. Hai, and B. Cheng, "Enhanced photocatalytic H2-production activity of TiO_2 by $Ni(OH)_2$ cluster modification," *Journal of Physical Chemistry C*, vol. 115, no. 11, pp. 4953–4958, 2010.

[19] J. Wang, J. Wu, Z. Zhang et al., "Sonocatalytic damage of bovine serum albumin (BSA) in the presence of nanometer anatase titanium dioxide (TiO_2)," *Ultrasound in Medicine and Biology*, vol. 32, no. 1, pp. 147–152, 2006.

[20] A. Di Paola, S. Ikeda, G. Marcì, B. Ohtani, and L. Palmisano, "Transition metal doped TiO_2: physical properties and photocatalytic behaviour," *International Journal of Photoenergy*, vol. 3, no. 4, pp. 171–176, 2001.

[21] H. Fu, L. Zhang, S. Zhang, Y. Zhu, and J. Zhao, "Electron spin resonance spin-trapping detection of radical intermediates in N-doped TiO_2-assisted photodegradation of 4-chlorophenol," *Journal of Physical Chemistry B*, vol. 110, no. 7, pp. 3061–3065, 2006.

[22] V. Iliev, D. Tomova, R. Todorovska et al., "Photocatalytic properties of TiO_2 modified with gold nanoparticles in the degradation of oxalic acid in aqueous solution," *Applied Catalysis A*, vol. 313, no. 2, pp. 115–121, 2006.

[23] R. Bacsa, J. Kiwi, T. Ohno, P. Albers, and V. Nadtochenko, "Preparation, testing and characterization of doped TiO_2 active in the peroxidation of biomolecules under visible light," *Journal of Physical Chemistry B*, vol. 109, no. 12, pp. 5994–6003, 2005.

[24] X. H. Li, J. B. Lu, Y. Dai, M. Guo, and B. B. Huang, "The synthetic effects of Iron with sulfur and fluorine on photoabsorption and photocatalytic performance in codoped TiO_2 ," *International Journal of Photoenergy*, vol. 2012, Article ID 203529, 8 pages, 2012.

[25] U. G. Akpan and B. H. Hameed, "The advancements in sol-gel method of doped-TiO_2 photocatalysts," *Applied Catalysis A*, vol. 375, no. 1, pp. 1–11, 2010.

[26] R. S. Sonawane and M. K. Dongare, "Sol-gel synthesis of Au/TiO_2 thin films for photocatalytic degradation of phenol in sunlight," *Journal of Molecular Catalysis A*, vol. 243, no. 1, pp. 68–76, 2006.

[27] H. Li, Z. Bian, J. Zhu, Y. Huo, H. Li, and Y. Lu, "Mesoporous Au/TiO_2 nanocomposites with enhanced photocatalytic activity," *Journal of the American Chemical Society*, vol. 129, no. 15, pp. 4538–4539, 2007.

[28] R. Cai, Y. Kubota, T. Shuin, H. Sakai, K. Hashimoto, and A. Fujishima, "Induction of cytotoxicity by photoexcited TiO_2 particles," *Cancer Research*, vol. 52, no. 8, pp. 2346–2348, 1992.

[29] E. Fabian, R. Landsiedel, L. Ma-Hock, K. Wiench, W. Wohlleben, and B. van Ravenzwaay, "Tissue distribution and toxicity of intravenously administered titanium dioxide nanoparticles in rats," *Archives of Toxicology*, vol. 82, no. 3, pp. 151–157, 2008.

[30] J. W. Xiong, L. Chen, M. S. Liu et al., "Optical manner for estimation viability of cells based on their morphological characteristics," *Journal of Optoelectronics Laser*, vol. 16, no. 12, pp. 1514–1518, 2005.

[31] A. Kathiravan and R. Renganathan, "Photoinduced interactions between colloidal TiO_2 nanoparticles and calf thymus-DNA," *Free Radical Biology and Medicine*, vol. 28, no. 7, pp. 1374–1378, 2009.

[32] A. P. Zhang and Y. P. Sun, "Photocatalytic killing effect of TiO_2 nanoparticles on Ls-174-t human colon carcinoma cells," *World Journal of Gastroenterology*, vol. 10, no. 21, pp. 3191–3193, 2004.

[33] D. E. J. G. J. Dolmans, A. Kadambi, J. S. Hill et al., "Vascular accumulation of a novel photosensitizer, MV6401, causes selective thrombosis in tumor vessels after photodynamic therapy," *Cancer Research*, vol. 62, no. 7, pp. 2151–2156, 2002.

[34] H. Hui, F. Dotta, U. Di Mario, and R. Perfetti, "Role of caspases in the regulation of apoptotic pancreatic islet beta-cells death," *Journal of Cellular Physiology*, vol. 200, no. 2, pp. 177–200, 2004.

[35] J. F. Reeves, S. J. Davies, N. J. F. Dodd, and A. N. Jha, "Hydroxyl radicals ($\cdot$OH) are associated with titanium dioxide (TiO_2) nanoparticle-induced cytotoxicity and oxidative DNA damage in fish cells," *Mutation Research*, vol. 640, no. 1-2, pp. 113–122, 2008.

[36] K. Yang, Y. Dai, and B. Huang, "Study of the nitrogen concentration influence on N-doped TiO_2 anatase from first-principles calculations," *Journal of Physical Chemistry C*, vol. 111, no. 32, pp. 12086–12090, 2007.

[37] X. Chen and S. S. Mao, "Titanium dioxide nanomaterials: synthesis, properties, modifications and applications," *Chemical Reviews*, vol. 107, no. 7, pp. 2891–2959, 2007.

[38] J. A. Rengifo-Herrera and C. Pulgarin, "Photocatalytic activity of N, S co-doped and N-doped commercial anatase TiO_2 powders towards phenol oxidation and *E. coli* inactivation under simulated solar light irradiation," *Solar Energy*, vol. 84, no. 1, pp. 37–43, 2010.

[39] Y. Kesong, D. Ying, H. Baibiao, and H. Shenghao, "Theoretical study of N-doped TiO_2 rutile crystals," *Journal of Physical Chemistry B*, vol. 110, no. 47, pp. 24011–24014, 2006.

[40] N. P. Huang, M. H. Xu, C. W. Yuan, and R. R. Yu, "The study of the photokilling effect and mechanism of ultrafine TiO_2 particles on U937 cells," *Journal of Photochemistry and Photobiology A*, vol. 108, no. 2-3, pp. 229–233, 1997.

[41] J. B. Lu, H. Jin, Y. Dai, K. S. Yang, and B. B. Huang, "Effect of electronegativity and charge balance on the visible-light-responsive photocatalytic activity of nonmetal doped anatase TiO_2 ," *International Journal of Photoenergy*, vol. 2012, Article ID 928503, 8 pages, 2012.

[42] W. H. Suh, K. S. Suslick, G. D. Stucky, and Y. H. Suh, "Nanotechnology, nanotoxicology, and neuroscience," *Progress in Neurobiology*, vol. 87, no. 3, pp. 133–170, 2009.